Topical Research Meeting: Prospects in Neutrino Physics (NuPhys2013) IOP Publishing
Journal of Physics: Conference Series **598** (2015) 012002 doi:10.1088/1742-6596/598/1/012002

Status of 3ν oscillation parameters at the end of 2013

F. Capozzi[1,2], G.L. Fogli[1,2], E. Lisi[2,*], A. Marrone[1,2], D. Montanino[3,4] and A. Palazzo[5]

[1]Dipartimento Interateneo di Fisica, Via Amendola 173, 70126 Bari, Italy
[2]Istituto Nazionale di Fisica Nucleare, Sezione di Bari, Via Orabona 4, 70126 Bari, Italy
[3]Dipartimento di Matematica e Fisica, Via Arnesano, 73100 Lecce, Italy
[4]Istituto Nazionale di Fisica Nucleare, Sezione di Lecce, Via Arnesano, 73100 Lecce, Italy
[5]Max-Planck-Institut für Physik, Föhringer Ring 6, 80805 München, Germany

[*]Speaker. Email: eligio.lisi@ba.infn.it

Abstract. Neutrino oscillation searches using a variety of sources (solar, atmospheric, accelerator and reactor neutrinos) have established a standard three-neutrino (3ν) mass-mixing framework and five of its parameters: the two squared mass gaps (δm^2, Δm^2) and the three mixing angles (θ_{12}, θ_{13}, θ_{23}). At present, a single class of experiments dominates each of these parameters, while only combined analyses of various (eventually all) data sets are needed to constrain the still unknown mass hierarchy [sign(Δm^2)], θ_{23} octant and CP-violating phase δ. We review the status of the known and unknown parameters — as emerging from a global analysis of the oscillation data available at the end of 2013 — and discuss the correlations and stability of the such parameters within different combinations of data sets.

1. Introduction

In just 15 years since the discovery of atmospheric neutrino oscillations, a new paradigm — the 3ν mass-mixing framework — has emerged in particle physics. Indeed, the vast majority of ν oscillation data can be explained by assuming that the three known flavor states $\nu_\alpha = (\nu_e, \nu_\mu, \nu_\tau)$ are mixed with three massive states $\nu_i = (\nu_1, \nu_3, \nu_3)$ via three mixing angles $(\theta_{12}, \theta_{13}, \theta_{23})$ and a possible CP-violating phase δ. The observed oscillations are driven by two independent differences between the squared masses m_i^2, which can be defined as $\delta m^2 = m_2^2 - m_1^2 > 0$ and $\Delta m^2 = m_3^2 - (m_1^2 + m_2^2)/2$, where $\Delta m^2 > 0$ and < 0 correspond to normal hierarchy (NH) and inverted hierarchy (IH), respectively.

At present (end of 2013), five of the above 3ν oscillation parameters have been measured, with an accuracy largely dominated by a specific class of experiments, namely: θ_{12} by solar data [1], θ_{13} by short-baseline (SBL) reactor data [2], θ_{23} by atmospheric data, mainly from Super-Kamiokande (SK) [3], δm^2 by long-baseline reactor data from KamLAND (KL) [2], and Δm^2 by long-baseline (LBL) accelerator data, mainly from MINOS [4] and T2K [5]. However, the mass hierarchy, the θ_{23} octant, and the CP-violating phase δ are still unknown.

In this context, global neutrino data analyses may be useful to assess the overall consistency and accuracy of the known parameters, as well as to squeeze possible hints about the unknown ones. In the following, we report and discuss the results of a recent global analysis which include all the data available at the time of this NuPhys Conference (December 2013) [6]. The reader is referred to [6] for further details and references not reported herein.

It should be noted that, in the 3ν framework, there are other unknowns not accessible to oscillation experiments, namely: the absolute neutrino mass scale [7, 8], the Dirac or Majorana nature of the neutrino fields [9, 10] and, in the latter case, the associated Majorana phases [9, 10, 11]. Current constraints on these unknowns, which are crucial for theoretical model building [10, 11, 12], will also be briefly commented below. Finally, it should be mentioned that some controversial results (not discussed herein) might indicate possible extensions of the above 3ν framework in terms of one or more additional mass states ν_j ($j \geq 4$), mostly sterile and with mass gaps at the (sub)eV scale. The reader is referred to [13] for an up-to-date discussion of the sterile neutrino phenomenology.

2. Global analysis: Methodology

In this Section we briefly discuss the various data sets and their combination in global fits.

LBL Acc. + Solar + KL data. The oscillation phenomenology of LBL accelerator experiments is dominated by the oscillation parameters (Δm^2, θ_{23}) in the $\nu_\mu \to \nu_\mu$ disappearance channel, supplemented by θ_{13} in the $\nu_\mu \to \nu_e$ appearance channel. However, the current accuracy of MINOS and T2K data requires that the oscillation probability is precisely calculated in terms of all the input parameters, including matter effects and subdominant terms driven by (δm^2, θ_{12}, δ). Since (δm^2, θ_{12}) are essentially fixed by the Solar and KL experiments, it makes sense to combine these data with LBL accelerator data from the very beginning. We remark that "Solar + KL" data provide a preference for $\sin^2\theta_{13} \sim 0.02$ in our analysis, which plays a role in the combination "LBL Acc. + Solar + KL," as discussed below.

Adding SBL reactor data. After the recent T2K observation of electron flavor appearance, the combination of LBL Acc. + Solar + KL data can provide a highly significant measurement of θ_{13} which, however, depends on the unknown CP violating phase δ and θ_{23} octant. SBL reactor experiments (Daya Bay, RENO, Double Chooz) provide (δ, θ_{23})-independent and accurate measurements of θ_{13}, which play a crucial role in the "LBL Acc. + Solar + KL + SBL Reac." combination.

Adding atmospheric neutrino data. Atmospheric data involve a very rich oscillation phenomenology in both appearance and disappearance modes involving ν_μ and ν_e. In principle, the high-statistics Super-Kamiokande experiment (phases I-IV) is thus sensitive to subleading effects related to the mass hierarchy, the θ_{23} octant and the CP phase δ. However, within the current experimental and theoretical systematic uncertainties, it remains difficult to disentangle and probe such small effects at a level exceeding $\sim 1\sigma$–2σ. Moreover, different and independent analyses of SK data, at comparable levels of refinement, do not necessarily provide similar hints about subleading effects. Therefore, we prefer to add these data only in the final "LBL Acc. + Solar + KL + SBL Reac. + SK Atm." combination, in order to separately gauge their effects on the various 3ν parameters.

Conventions for allowed regions. The data are compared to theoretical expectations via a refined χ^2 function which accounts for all known sources of correlated and uncorrelated uncertainties. In each of the above combined data analyses, the six oscillation parameters (Δm^2, δm^2, θ_{12}, θ_{13}, θ_{23}) are unconstrained in any given hierarchy (normal or inverted). Parameter ranges at N standard deviations are defined as $N\sigma = \sqrt{(\chi^2 - \chi^2_{\rm min})}$. This definition holds also in two-dimensional plots, where it is understood that the previous $N\sigma$ ranges are reproduced by projecting 2D contours over one parameter axis. All undisplayed parameters are marginalized away. Finally, the relative preference of the data for either NH or IH is measured by the quantity $\Delta\chi^2_{\rm I-N} = \chi^2_{\rm min}({\rm IH}) - \chi^2_{\rm min}({\rm NH})$, with the caveat that it cannot immediately be translated into "$N\sigma$" by taking the square root of its absolute value, because it refers to two discrete hypotheses [14].

3. Results on single oscillation parameters

In this Section we graphically report the results of our global analysis of increasingly richer data sets, grouped in accordance to the previous discussion, in terms of single oscillation parameters.

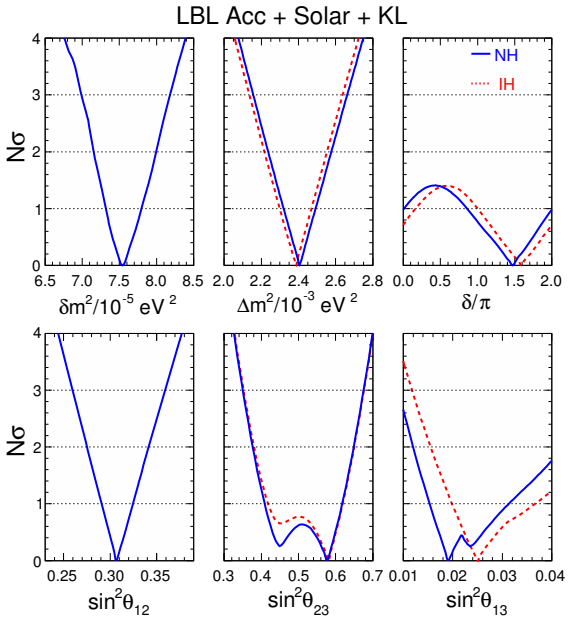

Figure 1. Combined 3ν analysis of LBL Acc. + Solar + KL data: Bounds on the oscillation parameters in terms of standard deviations $N\sigma$ from the best fit. Solid (dashed) lines refer to NH (IH). The horizontal dotted lines mark the 1σ, 2σ and 3σ levels for each parameter.

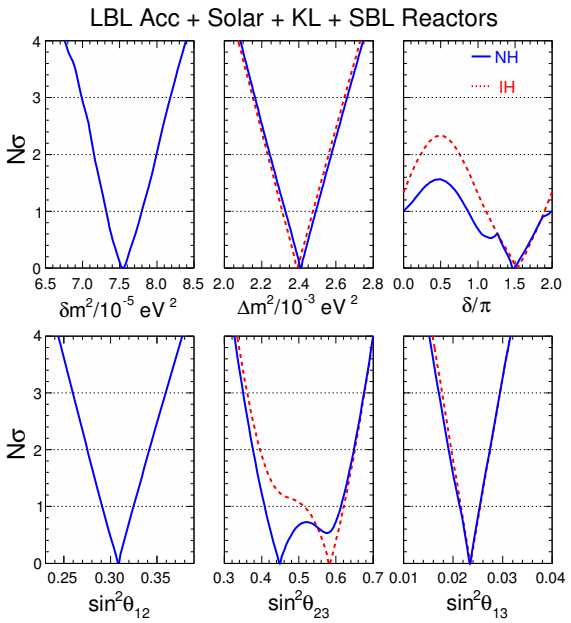

Figure 2. As in Fig. 1, but adding SBL reactor data.

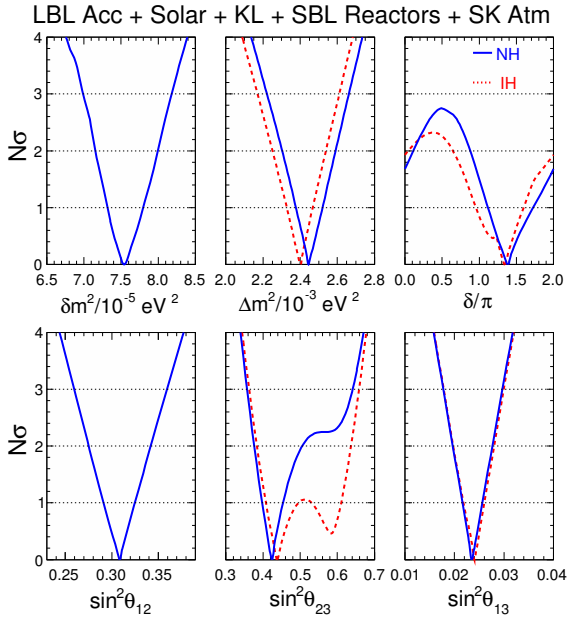

Figure 3. As in Fig. 2, but adding SK atmospheric data (global fit to all ν data).

Figures 1, 2 and 3 show the $N\sigma$ curves for the data sets defined in the previous section. In each figure, the solid (dashed) curves refer to NH (IH); the two curves basically coincide for the δm^2 and θ_{12} parameters, since they are determined by Solar+KL data which are largely insensitive to the hierarchy. For each parameter in Figs. 1–3, the more linear and symmetrical are the curves, the more gaussian is the associated probability distribution.

Figure 1 refers to the combination LBL Acc. + Solar + KL which, by itself, sets highly significant lower and upper bounds on all the oscillation parameters but δ. In this figure, the relatively strong appearance signal in T2K [5] dominates the lower bound on θ_{13}, and also drives the slight but intriguing preference for $\delta \simeq 1.5\pi$: indeed, for $\sin\delta \sim -1$, the CP-odd term in the $\nu_\mu \to \nu_e$ appearance probability is maximized. It should be noted that current MINOS appearance data generally prefer $\sin\delta > 0$ [4]; however, the stronger T2K appearance signal largely dominates in the global fit. On the other hand, MINOS disappearance data drive the slight preference for nonmaximal θ_{23}, as compared with nearly maximal θ_{23} in T2K [5]. The (even slighter) preference for the second θ_{23} octant is due to the interplay of LBL accelerator and Solar + KL data, as discussed in the next Section.

Figure 2 shows the results obtained by adding the SBL reactor data, which strongly reduce the θ_{13} uncertainty. Further effects of these data include: (*i*) a slightly more pronounced preference for $\delta \simeq 1.5\pi$ and $\sin\delta < 0$, and (*ii*) a swap of the preferred θ_{23} octant with the hierarchy ($\theta_{23} < \pi/4$ in NH and $\theta_{23} > \pi/4$ in IH). These features will be interpreted in terms of parameter covariances in the next Section.

Figure 3 shows the results obtained by adding the SK atmospheric data, thus obtaining the most complete data set. The main differences with respect to Fig. 2 include: (*i*) an even more pronounced preference for $\sin\delta < 0$, with a slightly lower best fit at $\delta \simeq 1.4\pi$; (*ii*) a slight reduction of the errors on Δm^2 and a relatively larger variation of its best-fit value with the hierarchy; (*iii*) a preference for θ_{23} in the first octant for both NH and IH, which is a persisting feature of our analyses. The effects (*ii*) and (*iii*) show that atmospheric neutrino data have the potential to probe subleading hierarchy effects, although they do not yet emerge in a stable or significant way. Table I summarizes in numerical form the results shown in Fig. 3.

In Figs. 1–3, an intriguing feature is the increasingly pronounced preference for nonzero CP violation with increasingly rich data sets, although the two CP-conserving cases ($\delta = 0, \pi$) remain allowed at $< 2\sigma$ in both NH and IH, even when all data are combined (see Fig. 3). It is worth noticing that the two maximally CP-violating cases ($\sin\delta = \pm 1$) have opposite likelihood: while the range around $\delta \sim 1.5\pi$ ($\sin\delta \sim -1$) is consistently preferred, small ranges around $\delta \sim 0.5\pi$ ($\sin\delta \sim +1$) appear to be disfavored (at $> 2\sigma$ in Fig. 3), In the next few years, the appearance channel in LBL accelerator experiments will provide crucial data to investigate these hints about ν CP violation [6], with relevant implications for models of leptogenesis [10].

From the comparison of Figs. 1–3 one can also notice a generic preference for nonmaximal mixing ($\theta_{23} \neq 0$), although it appears to be weaker than in our past analyses, essentially because the most recent T2K data prefer nearly maximal mixing, and thus "dilute" the opposite preference coming from MINOS and atmospheric data. Moreover, the indications about the octant appear to be somewhat unstable in different combinations of data. In the present analysis, only atmospheric data consistently prefer the first octant in both hierarchies, but the overall significance remains at the level $\sim 2\sigma$ in NH and is much lower in IH. These fluctuations show how difficult it is to reduce the allowed range of θ_{23}. In this context, the disappearance channel in LBL accelerator experiments will provide crucial data to address the issue of nonmaximal θ_{23} in the next few years [5, 15, 16].

Finally, we comment on the size of $\Delta\chi^2_{\rm I-N}$ which, by construction, is not apparent in Figs. 1–3. We find $\Delta\chi^2_{\rm I-N} = -1.3, -1.4, +0.3$, for the data sets in Figs. 1, 2, and 3, respectively. Unfortunately, such values are both small and with unstable sign, and do not provide us with any relevant indication about the hierarchy.

4. Selected parameter covariances

In this Section we show the allowed regions for selected couples of oscillation parameters, and discuss some interesting correlations.

Figure 4 shows the allowed regions in the plane ($\sin^2\theta_{23}$, $\sin^2\theta_{13}$). From left to right, the panels refer to increasingly rich data sets, while upper and lower panels refer to NH and IH, respectively. In the left panels, a slight negative correlation emerges from LBL appearance data, since the dominant oscillation amplitude contains a factor $\sin^2\theta_{23}\sin^2\theta_{13}$. The contours extend towards relatively large values of θ_{13}, especially in IH, in order to accommodate the relatively strong T2K appearance signal [5]. However, solar + KL data provide independent (although weaker) constraints on θ_{13} and, in particular, prefer $\sin^2\theta_{13} \sim 0.02$ in our analysis. This value is on the "low side" of the allowed regions and is thus responsible for the relatively high value of θ_{23} at best fit, namely, for the second-octant preference in both NH and IH. However, when current SBL reactor data are included in the middle panels, a slightly higher value of θ_{13} ($\sin^2\theta_{13} \simeq 0.023$) is preferred with very small uncertainties: this value is high enough to shift the best-fit of θ_{23} from the second to the first octant in NH, but not in IH. Finally, the inclusion of SK atmospheric data (right panels) provides in our analysis an overall preference for the first octant, which is however quite weak in IH. Unfortunately, as previously mentioned, the current hints about the θ_{23} octant do not appear to be particularly stable or convergent.

Figure 5 shows the allowed regions in the plane ($\sin^2\theta_{13}$, δ/π), which is at the focus of current research in neutrino physics. In the left panels there is a remarkable preference for $\delta \sim 1.5\pi$, where a compromise is reached between the relatively high θ_{13} values preferred by the T2K appearance signal, and the relatively low value preferred by solar + KL data. In the middle panel, SBL reactor data strengthen this trend by reducing the covariance between θ_{13} and δ. It is quite clear that we can still learn much from the combination of accelerator and reactor data in the next few years. Finally, the inclusion of SK atmospheric data in the right panels also adds some statistical significance to this trend, with a slight lowering of the best-fit value of δ.

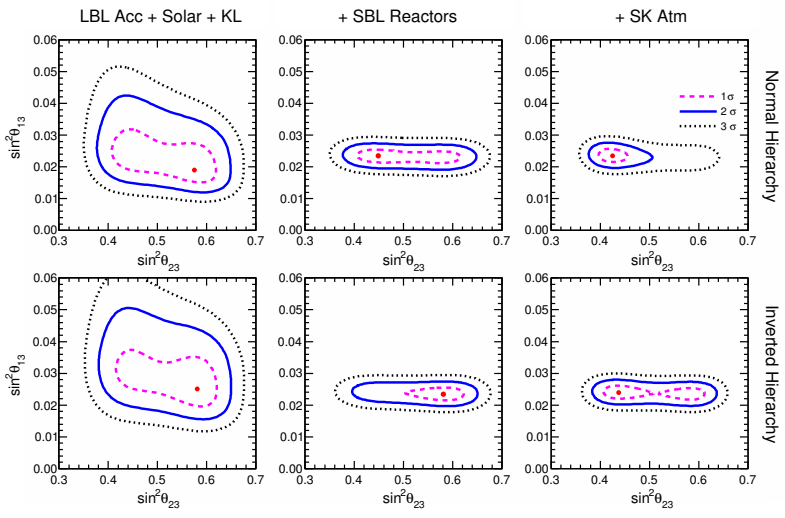

Figure 4. Results of the analysis in the plane charted by ($\sin^2\theta_{23}$, $\sin^2\theta_{13}$), all other parameters being marginalized away. From left to right, the regions allowed at 1, 2 and 3σ refer to increasingly rich datasets: LBL accelerator + solar + KamLAND data (left panels), plus SBL reactor data (middle panels), plus SK atmospheric data (right panels). Best fits are marked by dots. The three upper (lower) panels refer to normal (inverted) hierarchy.

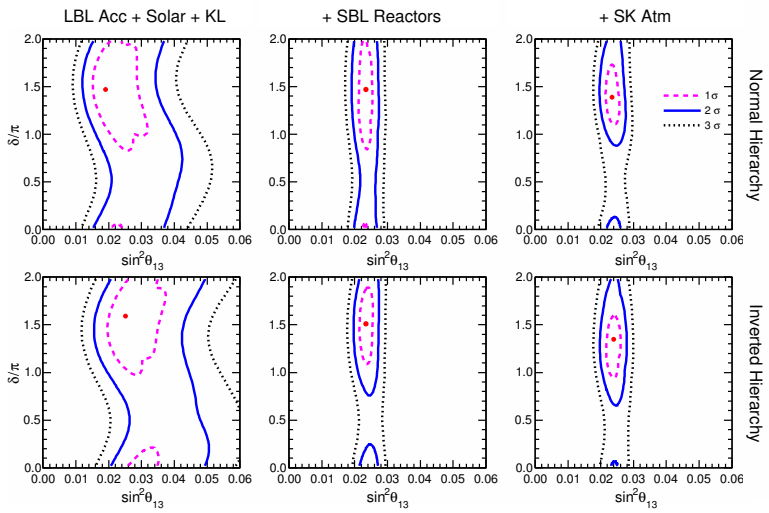

Figure 5. As in Fig. 4, but in the plane ($\sin^2\theta_{13}$, δ/π).

5. Implications on absolute neutrino mass observables

In general, absolute neutrino masses can be probed via three main methods. The first, classical one is provided by β decay, sensitive to the so-called "effective electron neutrino mass" m_β [7],

$$m_\beta = \left[\sum_i |U_{ei}|^2 m_i^2\right]^{\frac{1}{2}} = \left[c_{13}^2 c_{12}^2 m_1^2 + c_{13}^2 s_{12}^2 m_2^2 + s_{13}^2 m_3^2\right]^{\frac{1}{2}} \ . \tag{1}$$

The second observable — if neutrinos are Majorana spinors — is the effective "Majorana neutrino mass" $m_{\beta\beta}$ in $0\nu\beta\beta$ decay [9],

$$m_{\beta\beta} = \left|\sum_i U_{ei}^2 m_i\right| = \left|c_{13}^2 c_{12}^2 m_1 + c_{13}^2 s_{12}^2 m_2 e^{i\phi_2} + s_{13}^2 m_3 e^{i\phi_3}\right| \ , \tag{2}$$

where $\phi_{2,3}$ are additional unknown parameters (Majorana phases) [10]. Note that nuclear uncertainties might complicate the interpretation of possible future $0\nu\beta\beta$ signals [17]. The third observable is the sum of neutrino masses in standard cosmology [8]:

$$\Sigma = m_1 + m_2 + m_3 \ . \tag{3}$$

The oscillation constraints reported in the previous Section induce strong correlations among the above three main observables

Figure 6 shows such correlations in terms of 2σ constraints (bands) in the planes charted by any couple of the absolute mass observables. Note that the bands in the (m_β, Σ) plane of Fig. 6 are quite narrow, due to the high accuracy reached in the determination of all the oscillation parameters. In principle, precise measurements of (m_β, Σ) in the sub-eV range (where the bands for NH and IH branch out) could determine the mass spectrum hierarchy. In the two lower panels of Fig. 6, there remains a large vertical spread in the allowed slanted bands, as a result of the unknown Majorana phases in $m_{\beta\beta}$, which may interfere either constructively (upper part of each band) or destructively (lower part of each band). In principle, precise data in either the ($m_{\beta\beta}$, m_β) plane or the ($m_{\beta\beta}$, Σ) plane might thus provide constraints on the Majorana phases.

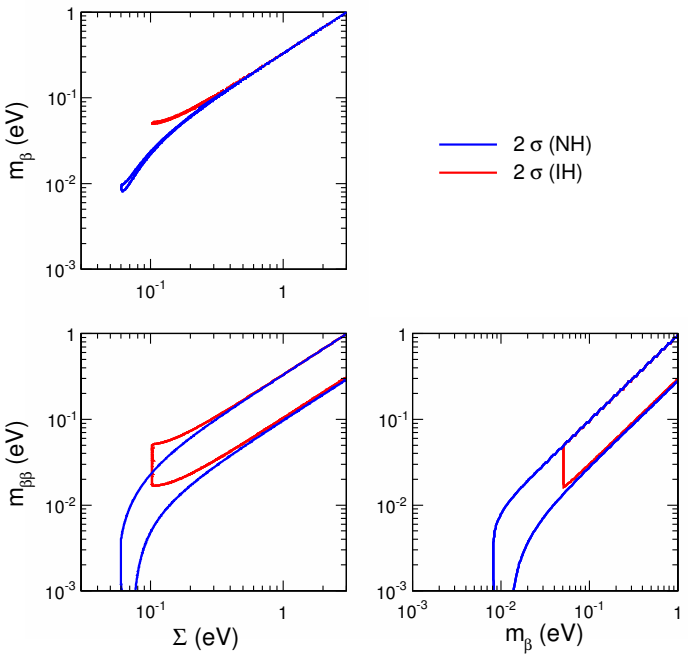

Figure 6. Constraints induced by oscillation data (at 2σ level) in the planes charted by any two among the absolute mass observables m_β (effective electron neutrino mass), $m_{\beta\beta}$ (effective Majorana mass), and Σ (sum of neutrino masses). Blue (red) bands refer to normal (inverted) hierarchy.

At present, there are only safe upper bounds on these absolute mass parameters, at the eV level for m_β [7], and in the sub-eV range for $m_{\beta\beta}$ [9] and Σ [8]. A great experimental activity is in progress towards mass sensitivity goals of $O(\sqrt{\Delta}m^2)$, at least via $0\nu\beta\beta$ and cosmological probes. Sensitivities of $O(\sqrt{\delta}m^2)$ in $0\nu\beta\beta$ decay appear to be extremely challenging at present.

In the most optimistic scenario, the absolute neutrino masses might be all around 0.1–0.2 eV, and thus observable in the next few years through measurements of at least two among the three (m_β, $m_{\beta\beta}$, Σ) parameters. Then, the concordance of two or three of these observables with the oscillation bands in Fig. 6 woul provide a fundamental cross-check of the standard framework with three massive and mixed neutrinos. If concordance is not achieved (e.g., if strong cosmological limits on Σ are not compatible with possible signals of $m_{\beta\beta} > 0$ within the bands of Fig. 6, or viceversa), the situation would become even more interesting from a phenomenological viewpoint. In this case, data might suggest modifications of the standard framework either in cosmology (e.g., adopting suitable variants of the concordance cosmological model) or in neutrino physics (e.g., exploring nonstandard mechanisms for $0\nu\beta\beta$ decay—a topic witnessing renewed interest). Conversely, the lack of a signal in any of the observables (m_β, $m_{\beta\beta}$, Σ) in the next few years would make the perspectives for the neutrino mass quest extremely challenging.

6. Conclusions

In the light of recent results coming from reactor and accelerator experiments, and of their interplay with solar and atmospheric data (as of December 2013), we have updated the estimated $N\sigma$ ranges of the known 3ν parameters (Δm^2, δm^2, θ_{12}, θ_{13}, θ_{23}), and we have revisited the status of the current unknowns [sign(Δm^2), sign($\theta_{23} - \pi/4$), δ]. The results of the global analysis of all data are shown in Fig. 3 in terms of single parameters. One can appreciate the high accuracy reached in the determination of the known oscillation parameters.

We have also discussed in some detail the status of the unknown parameters. Concerning the hierarchy [sign(Δm^2)], we find no significant difference between normal and inverted mass ordering. However, assuming normal hierarchy, we find possible hints about the other two unknowns, namely: a slight preference for the first θ_{23} octant, and possible indications for nonzero CP violation (with $\sin\delta < 0$), although at a level below $\sim 2\sigma$ in both cases. The second hint appears also in inverted hierarchy, but with even lower statistical significance.

In order to understand how the various constraints and hints emerge from the analysis, and to appreciate their (in)stability, we have considered increasingly rich data sets, starting from the combination of LBL accelerator plus solar plus KamLAND data, then adding SBL reactor data, and finally including atmospheric data. We have discussed the fit results both on single parameters and on selected couples of correlated parameters. It turns out that the hints about the θ_{23} octant appear somewhat unstable at present, while those about δ (despite being statistically weaker) seem to arise from an intriguing convergence of several pieces of data.

Finally, we have discussed the implication of such results for the three observables sensitive to absolute neutrino masses via single- and double-beta decay and cosmology. In general, global analyses of oscillation and non oscillation data appear to provide valuable tools to gauge the overall consistency of the data in a given framework (assumed to be standard 3ν mixing herein). Further experimental data might either confirm the 3ν framework and fix its remaining unknowns (possible CP violation, θ_{23} octant, absolute masses and their ordering, Dirac versus Majorana nature, and Majorana phases in the latter case), or find interesting discrepancies which would require new physics beyond the three known neutrino states and their standard interactions.

Acknowledgments

E.L. is grateful to the organizers, F. Di Lodovico and S. Pascoli, for their kind invitation and hospitality in London, and for their fine organization of a most informative and enjoyable conference. This work is supported in part through the Theoretical Astroparticle Physics Research Programs by the Italian Istituto Nucleare di Fisica Nucleare (INFN TAsP Initiative) and Ministero dell'Istruzione, Università e Ricerca (MIUR PRIN Project).

References

[1] M. Pallavicini, talk at this Conference.
[2] Y. Wang, talk at this Conference.
[3] S. Soldner-Rembold, talk at this Conference.
[4] C. Backhouse, talk at this Conference.
[5] T. Nakaya, talk at this Conference.
[6] F. Capozzi, G. L. Fogli, E. Lisi, A. Marrone, D. Montanino and A. Palazzo, "Status of three-neutrino oscillation parameters, circa 2013," preprint arXiv:1312.2878v1 [hep-ph]. The results shown herein refer to v1 of this preprint, including all 2013 neutrino data. A second version of this preprint [arXiv:1312.2878v2], including T2K data appeared in 2014, has been published on Phys. Rev. D **89**, 093018 (2014).
[7] G. Drexlin, talk at this Conference.
[8] L. Verde, talk at this Conference.
[9] M. Chen, talk at this Conference.
[10] S. Petcov, talk at this Conference.
[11] F. Feruglio, talk at this Conference.
[12] F. Deppisch, talk at this Conference.
[13] J. Kopp, talk at this Conference.
[14] A. Tonazzo, talk at this Conference.
[15] R. Wilson, talk at this Conference.
[16] D. Wark, talk at this Conference.
[17] F. Simkovic, talk at this Conference.